Charging Coordination and Load Balancing of Plug-in Electric Vehicles in Unbalanced Low-Voltage Distribution Systems

Kikhanadi, Mohammad Reza ; Hajizadeh, Amin; Shahirinia, Amir

Charging coordination and load balancing of plug-in electric vehicles in unbalanced low-voltage distribution systems

Mohammad Reza Kikhavani[1], Amin Hajizadeh[2] ✉, Amir Shahirinia[3]

[1]Department of Electrical and Robotic Engineering, Shahrood University of Technology, 3619995161 Shahrood, Iran
[2]Department of Energy Technology, Aalborg University, 6700 Esbjerg, Denmark
[3]Department of Electrical Engineering, University of the District of Columbia, Washington DC, 20008, USA
✉ E-mail: aha@et.aau.dk

Abstract: Plug-in electric vehicles (PEVs) are gaining popularity as a solution to reduce greenhouse gas production. On the other hand, uncoordinated charging of PEVs is a reason for grid stress and increasing congestion, total power consumption (TPC) and distribution lines and transformers losses. Moreover, single-phase connection of electric vehicles in residential buildings causes line current imbalance and it has more negative effects on TPC and power losses. Thus, they are characterised as unbalanced loads with random locations, plug-in times, charging rates, and durations. Hence, a charging coordination algorithm is proposed to utilise the integration of PEVs in both operational modes (grid-to-vehicle, vehicle-to-grid) to guarantee power loss reduction, voltage profile maintaining and load current balancing. The introduced algorithm can perform an optimal calculation to determine proper phase for PEVs in distribution feeders and decline the unbalancing by deploying a new device called phase switcher which is in series with chargers in residential buildings. The phase switcher is connected to the smart load management centre which uses the proposed algorithm to determine the proper phase for connection or disconnection of PEVs and finding the appropriate numbers of PEVs. To show the effectiveness of the proposed algorithm, simulation results are provided.

Nomenclature

n	total number of feeders
i	feeder number
$P_{\Delta t}^{\text{total demand(1)}}$	power consumption in each time step (W)
$P_{\Delta t}^{B-\text{load}}$	power consumption of base load in each time step (W)
$P_{\Delta t}^{\text{EV}-\text{load}}$	power consumption of electric vehicle (EV) load in each time step (W)
$P_{\Delta t}^{\text{loss}}$	total network power losses in each time step (W)
$P_{\Delta t}^{B-\text{loss}}$	base load power losses in each time step (W)
$P_{\Delta t}^{\text{EV}-\text{loss}}$	plug-in EVs (PEVs) load power losses in each time step (W)
$P_{\Delta t}^{\text{line}-\text{loss}}$	lines power losses in each time step (W)
$P_{\Delta t}^{\text{trans}-\text{loss}}$	transformers power losses in each time step (W)
$P_{\Delta t}^{\text{ave}}$	average power in three-phase lines in each time step (W)
P_i	power consumption of EVs in every feeder,
N_{G2V}	number of EVs including [grid-to-vehicle (G2V)]
N_{V2G}	number of PEVs including vehicle-to-grid (V2G)
N_{exch}	exchange amount of EV in each phase
$D_{\Delta t, \max}$	network maximum power demand
V_{spec}	nominal voltage of grid (p.u.)
$\Delta V^{\max}$	maximum deviations of voltage (p.u.)
V_{ph}	phase voltage (p.u.)
$N_{\text{ex}-1}$	number of EVs that must be plugged out
F	compensation factor
α_1 and α_2	weight factors
β_1 and β_2	weight factors

1 Introduction

The engagement of electric vehicles (EVs) is growing as a solution for global warming reduction and the diminution of air pollution. EVs are capable of increasing energy efficiency and declining fossil fuel dependence in transportation systems [1]. In the beginning, plug-in EVs (PEVs) were only connected to the grid for battery charging. However, new smart grid services are offering the flexibility of energy discharge to the grid and are technically named as vehicle-to-grid (V2G) mode and grid-connected PEVs practically operate as mobile energy storage [2]. Different PEV situations and charging coordination methods are considered to examine the impact of PEVs on distribution systems [3]. The work reported in [3] describes the effect of charging strategies on the load profile. Different PEV penetration levels are considered in [4] to estimate the PEV impact on system power losses. Pazouki *et al*. [5] evaluated the PEVs charging effect on distribution transformer aging in the presence of rooftop solar photovoltaic (PV) systems. The effect of charging on low-voltage residential distribution systems is studied in [6] with a case study for the year 2030. In [7], different charging strategies are proposed and impact on daily peak loads is examined. Luo *et al*. [8] evaluated the additional investments for different PEV penetration levels along with power losses. Apart from the negative impacts on voltage and power losses, the authors of [9, 10] also focused on PEV impact on distribution system reliability. Surprisingly, the V2G operation mode is not considered for reliability evaluation of the system. EVs' impact on power system reliability is examined in [11]. Some researchers have focused on the mitigation of PEV impact on distribution systems in [12–14]. Tal *et al*. [12] have offered real-time smart load management control strategy for reduction of power losses and voltage profile improvement. Reactive power control is implemented in charging stations to develop the voltage profile in [13]. The integration of distributed generations (DGs) has proved their reliability [15] and techno-economic benefits [16]. Thus, DGs integration has been considered as a worthy solution to compensate for the PEVs charging impacts [17]. The charging demand for PEVs is mitigated by using PV units in an unbalanced distribution system [18]. With considerations in cost, reliability, power losses and voltage profile, synchronised scheduling of charging stations and DGs is studied in [19]. Furthermore, the capacity-boosting with DGs is proposed to compensate for the increasing PEVs penetration in [20]. The design of charging stations integrated with wind generation and storage is explored in

[21]. In [22], the optimal penetration level of DGs is assessed for a predefined PEV penetration level. In the literature, most of the research is concentrated on the study of PEVs impact on power consumption and power losses. Moreover, most of the literature has presented the charging coordination of PEVs in a balanced condition. In low-voltage distribution systems, the unbalanced condition is one of the main challenges for distribution system operator. Load balancing (LB) is one of the major power quality problems in LV distribution networks. PEVs can increase network LB since they are relatively huge single-phase load/generator units. Although LB due to PEVs was discussed in [23, 24], it was not studied entirely. The design of charging stations integrated with wind generation and storage is discussed in [25]. In [26], the optimal penetration level of DGs is estimated for a predefined PEV penetration level. The effect of charging/discharging levels and location of PEVs were not considered in these studies. The V2G and ground-to-vehicle (G2V) operation modes were also not investigated thoroughly for LB analysis. Investigating LB due to PEVs in the network is the main contribution of this study. This investigation is of great interest since the random connection point of PEVs among the three phases of the LV residential network, in addition to their charging levels (in G2V mode) and their output power (in V2G mode), might increase network LB. Therefore, in this study, the integration of PEVs is utilised as a valuable opportunity in order to satisfy power loss reduction, voltage profile maintaining and performing load current balancing. The proposed algorithm can perform optimal programming to determine proper phase for EVs (G2V, V2G) in distribution feeders and by load unbalancing in the network. All three-phase parameters have been chosen based on the balanced situation of the network. Therefore, unbalancing has been declining with the presence of EVs. Obviously, there is a new idea based on the utilisation of a new device called a phase switcher (PS) that is in series with chargers in homes. This device can change the connected phase of chargers, as both switchers and chargers, which is linked to a smart load management centre (SLMC) to exchange signals and commands. In fact, the source of unbalancing relates to unbalanced loads and the difference in the number of customers on three-phase (R, S, T) of distribution transformers that lead to load current amplitude balancing (not angle) in a three-phase system.

The paper is organised as follows: in Section 2, the proposed algorithm and mathematical formulation of coordinated charging are presented. Then in Section 3, the simulation results and discussion are explained which are obtained from the real distribution system [27, 28]. Moreover, different scenarios are given to prove the importance of the offered algorithm.

2 Suggested algorithm and formulations of EVs (G2V, V2G) charging

This section includes formulations of PEV charging, objective functions, network constraints, our suggested algorithm, formulations of phase balancing, maximum sensitivity selection (MSS) optimisation and scenarios of EVs presence.

2.1 Formulations of charging and objective functions and network conditions

According to the main assumption of unbalanced loads, all equations have been defined as three-phase and it means that losses, basic loads, and EVs loads are separated for each phase (R, S, T). Also, for primary purposes [28], there are two conditions concerning total power consumption (TPC) and voltage limitations. The first condition is used to reduce power losses by controlling plugging in and plugging out of EVs (G2V) and the second condition is used to improve the voltage profile in each node by considering the presence of EVs (G2V). Equations (1)–(4) are defined when EVs are plugged in. Equation (5) presents the polarity of EVs power based on the number of EVs (G2V, V2G) in each phase. However, the main purpose relates to LB, which can be seen in (6)–(9). Equation (6) includes several terms such as power losses, average voltage deviation and additional power of each phase, which is further described in (7)–(9). Equation (9) is the

calculation of the average power of phases in each time step and (10) and (11) indicate network limitations

$$
\begin{aligned}
P_{\Delta t, R}^{\text{total demand}(1)} &= P_{\Delta t, R}^{\text{B-load}} + P_{\Delta t, R}^{\text{loss}(1)}, \\
P_{\Delta t, S}^{\text{total demand}(1)} &= P_{\Delta t, S}^{\text{B-load}} + P_{\Delta t, S}^{\text{loss}(1)}, \\
P_{\Delta t, T}^{\text{total demand}(1)} &= P_{\Delta t, T}^{\text{B-load}} + P_{\Delta t, T}^{\text{loss}(1)}, \\
P_{\Delta t}^{\text{total demand}(1)} &= \sum_{i=R,S,T} P_{\Delta t, i}^{\text{total demand}(1)},
\end{aligned}
\tag{1}
$$

$$
\begin{aligned}
P_{\Delta t, R}^{\text{loss}(1)} &= P_{\Delta t, R}^{\text{B-loss}} = P_{\Delta t, R}^{\text{line-loss}(1)} + P_{\Delta t, R}^{\text{trans-loss}(1)}, \\
P_{\Delta t, S}^{\text{loss}(1)} &= P_{\Delta t, S}^{\text{B-loss}} = P_{\Delta t, S}^{\text{line-loss}(1)} + P_{\Delta t, S}^{\text{trans-loss}(1)}, \\
P_{\Delta t, T}^{\text{loss}(1)} &= P_{\Delta t, T}^{\text{B-loss}} = P_{\Delta t, T}^{\text{line-loss}(1)} + P_{\Delta t, T}^{\text{trans-loss}(1)},
\end{aligned}
\tag{2}
$$

$$
\begin{aligned}
P_{\Delta t, R}^{\text{total demand}(2)} &= P_{\Delta t, R}^{\text{B-load}} + P_{\Delta t, R}^{\text{EV-load}} + P_{\Delta t, R}^{\text{loss}(2)}, \\
P_{\Delta t, S}^{\text{total demand}(2)} &= P_{\Delta t, S}^{\text{B-load}} + P_{\Delta t, S}^{\text{EV-load}} + P_{\Delta t, S}^{\text{loss}(2)}, \\
P_{\Delta t, T}^{\text{total demand}(2)} &= P_{\Delta t, T}^{\text{B-load}} + P_{\Delta t, T}^{\text{EV-load}} + P_{\Delta t, T}^{\text{loss}(2)}, \\
P_{\Delta t}^{\text{total demand}(2)} &= \sum_{i=R,S,T} P_{\Delta t, i}^{\text{total demand}(2)}
\end{aligned}
\tag{3}
$$

$$
\begin{aligned}
P_{\Delta t, R}^{\text{loss}(2)} &= P_{\Delta t, R}^{\text{B-loss}} + P_{\Delta t, R}^{\text{EV-loss}} = P_{\Delta t, R}^{\text{line-loss}(2)} + P_{\Delta t, R}^{\text{trans-loss}(2)}, \\
P_{\Delta t, S}^{\text{loss}(2)} &= P_{\Delta t, S}^{\text{B-loss}} + P_{\Delta t, S}^{\text{EV-loss}} = P_{\Delta t, S}^{\text{line-loss}(2)} + P_{\Delta t, S}^{\text{trans-loss}(2)}, \\
P_{\Delta t, T}^{\text{loss}(2)} &= P_{\Delta t, T}^{\text{B-loss}} + P_{\Delta t, T}^{\text{EV-loss}} = P_{\Delta t, T}^{\text{line-loss}(2)} + P_{\Delta t, T}^{\text{trans-loss}(2)},
\end{aligned}
\tag{4}
$$

$$
\begin{aligned}
N_{\text{G2V}-R} > N_{\text{V2G}-R} &\rightarrow P_{\Delta t-R}^{\text{EV-load}} > 0 \\
N_{\text{G2V}-S} > N_{\text{V2G}-S} &\rightarrow P_{\Delta t-S}^{\text{EV-load}} > 0 \\
N_{\text{G2V}-T} > N_{\text{V2G}-T} &\rightarrow P_{\Delta t-T}^{\text{EV-load}} > 0 \\
N_{\text{G2V}-R} < N_{\text{V2G}-R} &\rightarrow P_{\Delta t-R}^{\text{EV-load}} < 0 \\
N_{\text{G2V}-S} < N_{\text{V2G}-S} &\rightarrow P_{\Delta t-S}^{\text{EV-load}} < 0 \\
N_{\text{G2V}-T} < N_{\text{V2G}-T} &\rightarrow P_{\Delta t-T}^{\text{EV-load}} < 0
\end{aligned}
\tag{5}
$$

Objective functions

$$
\text{Min}\left(\sum_{i=R,S,T} P_{\Delta t, i}^{\text{loss}(2)} + |\Delta V_{\text{ave}}| + \sum_{i=R,S,T} P_{\text{add}-i} \right)
\tag{6}
$$

$$
V_{\text{ave}} = \left(\frac{1}{n} \sum_{i=1}^{n} V_i \right) = \frac{V_1 + V_2 + \cdots + V_n}{n}
$$

$$
\begin{aligned}
\text{Min}|\Delta V_i| &\simeq \text{Min}|\Delta V_{\text{ave}}| \simeq \text{Min}|V_{\text{ave}} - V_{\text{spec}}| \\
&= \text{Min}\left| \left(\frac{1}{n} \sum_{i=1}^{n} V_i \right) - V_{\text{spec}} \right| \\
&= \text{Min}\left(\frac{1}{n} \sum_{i=1}^{n} |1 - V_i| \right) = \text{Min}\left(\frac{1}{n} \sum_{i=1}^{n} |\Delta V_i| \right)
\end{aligned}
\tag{7}
$$

$$
\begin{aligned}
P_{\text{add}-R} &= |P_{\Delta t, \text{ave}} - P_{\Delta t, R}^{\text{total demand}(2)}| \\
P_{\text{add}-S} &= |P_{\Delta t, \text{ave}} - P_{\Delta t, S}^{\text{total demand}(2)}| \\
P_{\text{add}-T} &= |P_{\Delta t, \text{ave}} - P_{\Delta t, T}^{\text{total demand}(2)}|
\end{aligned}
\tag{8}
$$

$$
P_{\Delta t, \text{ave}} = \frac{\sum_{i=R,S,T} P_{\Delta t, i}^{\text{total demand}(2)}}{3} = \frac{P_{\Delta t}^{\text{total demand}(2)}}{3}
\tag{9}
$$

Subject to

$$
V^{\min} \leq V_{\text{ph}, i} \leq V^{\max}; \quad \text{ph} = R, S, T; \quad i = 1, \ldots, n
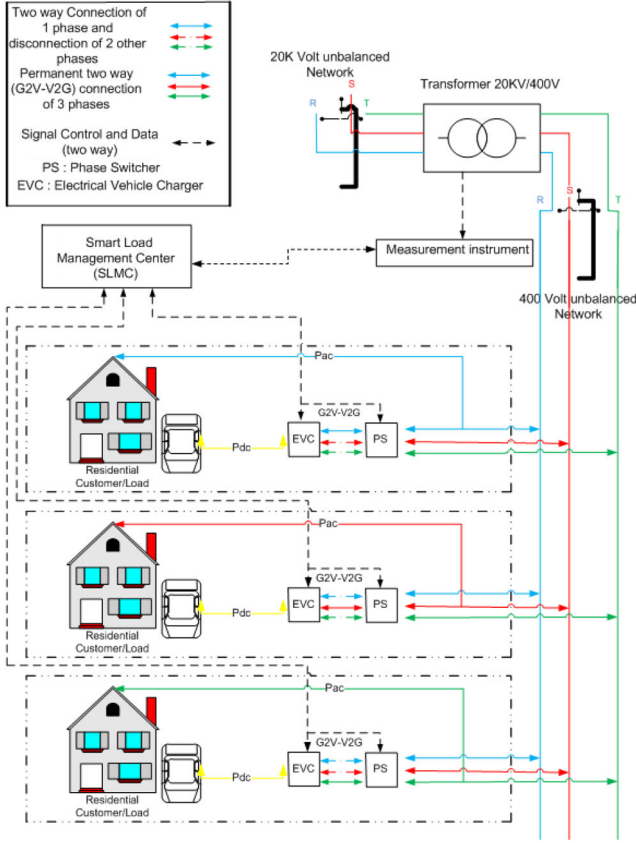\tag{10}
$$

Fig. 1 *General overview of the unbalanced network, PEV, homage chargers, and SLMC*

$$P_{\Delta t}^{\text{total demand}(2)} = P_{\Delta t}^{\text{B-load}} + P_{\Delta t}^{\text{EV-loss}} + P_{\Delta t}^{\text{loss}} \leq D_{\Delta t, \text{Max}} \quad (11)$$

2.2 Overview of the suggested algorithm and SLMC

The overview of three-phase unbalanced grids and the SLMC can be seen in Fig. 1. In unbalanced grids, the residential loads are connected to the 400-volt grid as single-phase load and PEVs (G2V–V2G) exchange energy with the distribution network through home PEV chargers and PSs. Here, it is assumed the single-phase standard EV charger is employed in all homes and a fast charger condition has not been considered. Also, the SLMC runs the suggested algorithm and monitors the loads. There is a two-way connection between SLMC and all elements of the grid such as chargers, PSs, loads and transformers through measurement instruments. Moreover, the SLMC receives real-time information from different parts of the system such as three-phase power consumption (TPPC), three-phase voltage profile of nodes and phase sequence and presence of EVs. Next, the algorithm determines the phase sequence of EVs based on previously analysed imported data and does permanent planning of the presence of EVs (G2V–V2G). From there, the SLMC sends commands to chargers and PSs that determine the chargers' connection status to the grid and phase of the switchers (chosen among R, S or T) in order to balance loads. Undoubtedly, it is assumed that there is smart commutations equipment for transmission information. In Fig. 2, the suggested algorithm has been presented. Remarkably, the algorithm of our last paper has been modified and a new one has two stages with considerable abilities. The first stage is to keep grid constraints (TPC, maximum deviations of voltage) and most importantly, the second stage determines phase sequence (LB). The time step is 15 min and is treated as real-time optimisation where both stages occur. In the first stage, all imported data such as TPPC and number of PEVs (G2V–V2G) in each time step are received and analysed. After that, power flow with the presence of EVs is performed and then sorted in vector-based sensitive optimisation. Then, the mentioned algorithm checks grid limitations.

If TPC limitation is violated, it shall defer the charging time of several EVs (G2V) to the next time step (plug out these EVs) in order to decrease TPC. The objective is to plug out the minimum number of EVs with the most effect on TPC and losses (3–5). Then, the voltage limitation shall be checked – if there is any violation in each feeder, the algorithm plugs out EVs (G2V–V2G) of that feeder until the next time step. This method is done as one by one and performs power flow after the voltage constraints are checked again. Formulas (12) and (13) calculate the approximate number of EVs (G2V)

$$P_{\Delta t}^{\text{total}} - D_{\Delta t}^{\text{max}} = P_{\text{ex}} \quad (12)$$

$$N_{\text{ex}-2} = N_{\text{ex}-1} \times FN_{\text{ex}-1} = \frac{P_{\text{ex}}}{2.079(\text{kW})} \quad (13)$$

The difference between the network's maximum demand and network power consumption is defined as P_{ex}. F can range from 0.9 to 0.95 based on total losses because of EV charging [27, 28]. In this method, accelerating the algorithm operation as the number of load flow computation has in each time step (real time), especially when large numbers of EVs are ready to plug in [28].

2.3 Performance of MSS optimisations in the suggested algorithm

As it seems, the MSS has two terms: the power losses sensitivity to variations of EVs power and the average voltage sensitivity to variations of EVs power for each feeder that has EVs. The optimisation problem with discrete variables deals with the main coordination problem of PEVs (G2V, V2G) in the presence of linear and non-linear loads. EVs can connect to a network as soon as possible by performing this method while providing attention to priority-charging time zones. The existence of EVs in every feeder has a direct effect on the voltage profile of all feeders. Therefore, the adding phase of average voltage sensitivity to the initial phrase has a direct effect on EVs' presence and priority in the network. After calculation of MSS for each EV's feeder (G2V) in each time step (with utilisation of the Jacobin entries [29]), the EVs are sorted in a vector of decreasing order (EVs have presence priority based on this vector). The vector is sorted such that EVs (G2V) which have more effect on soaring losses and distortion of voltage have more priority for disconnecting (plugging out). The maximum sensitivity analysis is calculated with the usage of partial derives as follows: (see (14))

2.4 Method and formulations of phase balancing

Using Figs. 3 and 4 as samples, the effect of phase change of EVs (G2V–V2G) on the power consumption of different phases are clear in two states. Before utilisation of our algorithm (Fig. 2) in the first state, the average power is higher than two phases and EVs (G2V–V2G) that are connected to the grid through different phases in stage 1. After the utilisation of the algorithm and EV phase changes, the power consumption of a different phase is close to P_{ave} in stage 2. What is clear is that the number of residential loads (homes) is the same in the two states. Equations (15)–(18) calculates additional powers of each phase and the number of EVs which plug out of the grid in the first state. The changing of EVs number of each phase and their powers are presented in (19)–(23) through two stages. The additional powers and unbalanced distances of three phases have been shown in the first stage in (19) and then presented in the second stage in (20). The number of EVs, which are charged, is calculated in (21) and (22) (first state: $P_x < P_{\text{ave}}$, $P_y > P_{\text{ave}}$, $P_z > P_{\text{ave}}$). After that, the relations and exchanging of EVs (G2V–V2G) throughout different phases are demonstrated in (23). These equations have shown trends of LB that the changing of all phases is coordinated, and the phase of each EV is determined in order to reduce unbalanced distant between powers of phases and average power. The showing of two stages is an example to demonstrate the changing trends of LB. All events that have occurred in two stages are presented in Fig. 3. Finally, the optimal goal is to reduce additional powers of different
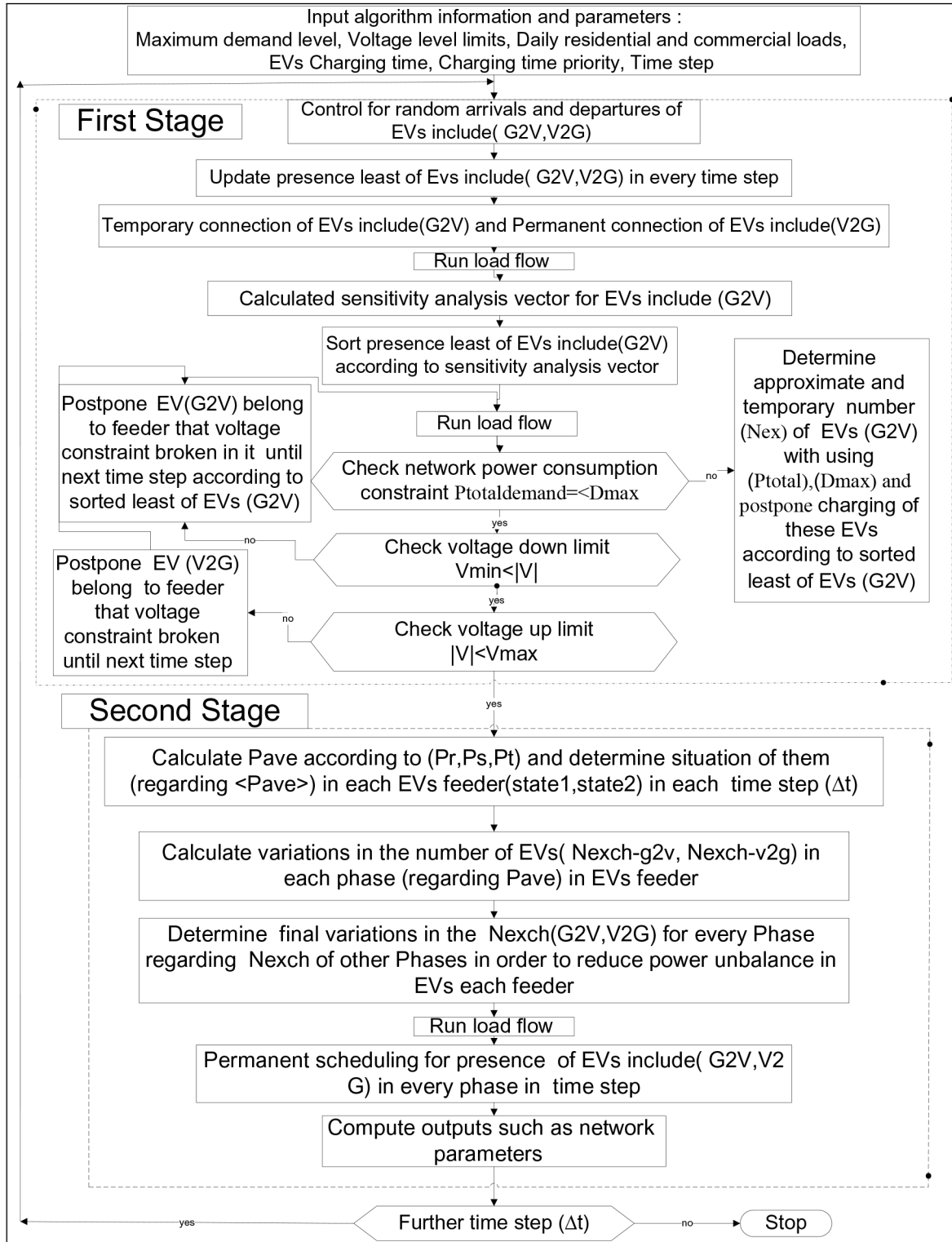
Fig. 2 *First and second stages of the suggested algorithm for coordination charging and phase balancing*

phases towards zero and power consumption (PC) of phases are equal to average power, as this issue has been proved in (24)–(27). The factors β_1 and β_2 are weight factors, which are used for phase changing of EVs between different phases. The number of factors depends on the PC of phases and N_{G2V}, N_{V2G} of phases. Similarly,

in the second state shown in Fig. 4, the average power is less than the second phase in the first stage. After changing the phase of EVs, the PC of a different phase is close to pave (second state: $P_x < P_{ave}$, $P_y < P_{ave}$, $P_z > P_{ave}$). The additional powers of each phase and the number of EVs (plugging out) are presented in (15)–

$$
\begin{aligned}
\mathrm{MSS}_i &= \left(\alpha_1 \times \frac{\partial P_{\mathrm{loss}}}{\partial P_i} \right) + \left(\alpha_2 \times \frac{\Delta |V_{\mathrm{ave}}|}{\Delta P_i} \right) \\
&= \left(\alpha_1 \times \frac{\partial P_{\mathrm{loss}}}{\partial P_i} \right) + \left(\alpha_2 \times \frac{1}{n} \left(\frac{\Delta |V_i|}{\Delta P_i} + \cdots + \frac{\Delta |V_i|}{\Delta P_i} + \cdots + \frac{\Delta |V_n|}{\Delta P_i} \right) \right) \\
\alpha_1 + \alpha_2 &= 1, \quad \alpha_1 = \alpha_2 = 0.5
\end{aligned}
\tag{14}
$$

Fig. 3 *General view of the first stage of the phase balancing process in residential feeders*
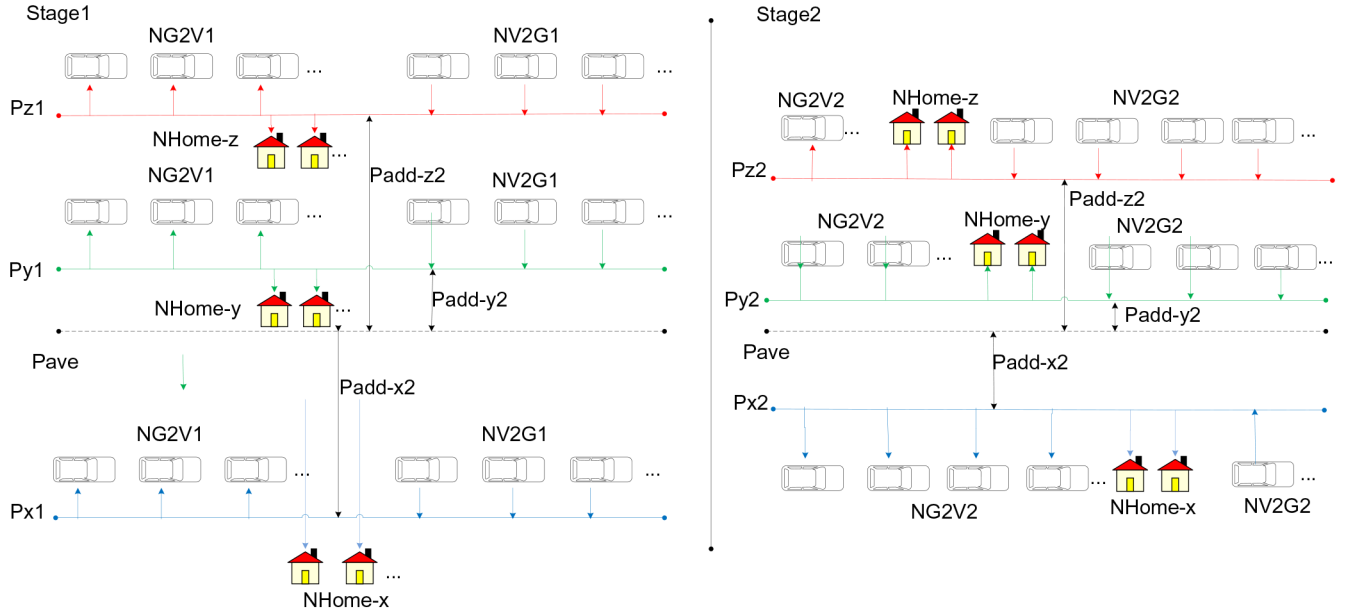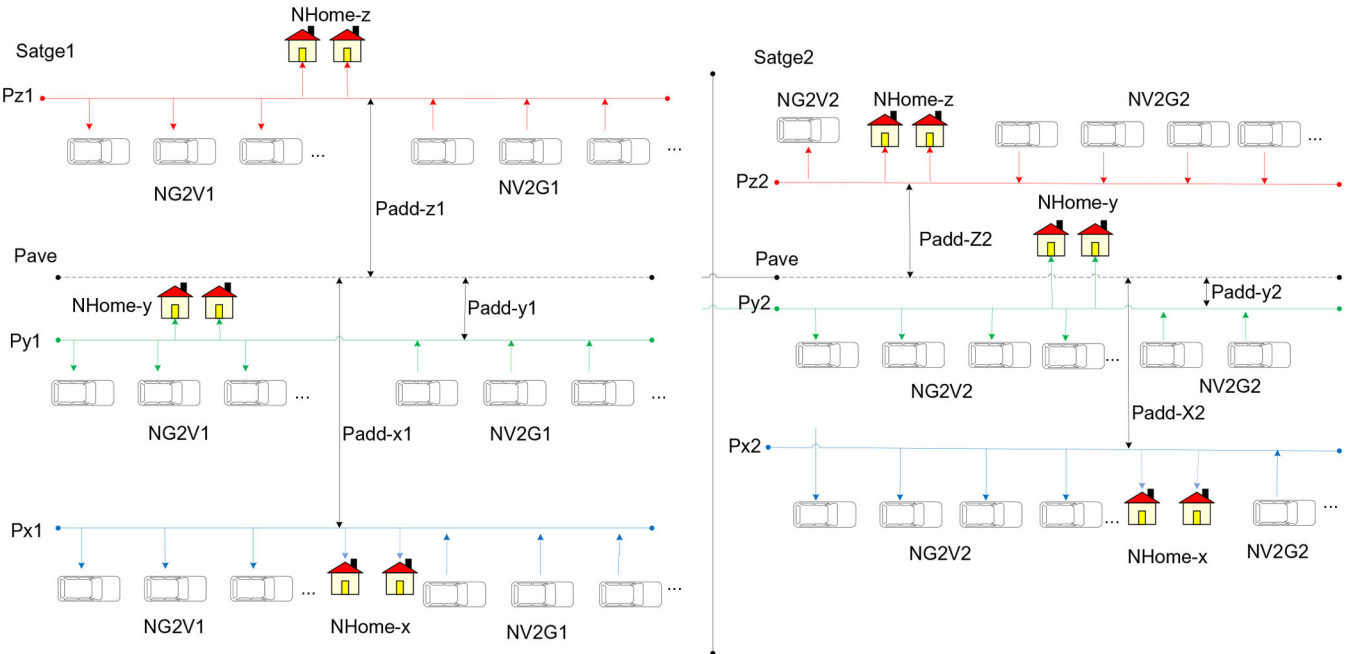

Fig. 4 *General view of the second stage of the phase balancing process in residential feeders*

(17). Like the last state, (28)–(32) calculate mentioned parameters in two-stage of the second state.

Again, the number of residential loads (homes) in two stages is equal. In fact, the position of middle phase (according to pave) determines the direction of phase changing of EVs (G2V–V2G) and by reducing additional power (P_{add}), a smaller number of EVs need change phase. In the final stage (ideal), (33) has shown the final amount of PC of each phase is equal to average power (P_{ave}). Also, (34)–(36) indicate limitations on final changing of EVs number. As it seems, in two states, EVs (G2V) are moved from up phases ($P > P_{ave}$) to down phases ($P < P_{ave}$) in order to reduce power in up phases and increase power in down phases. On the other hand, EVs (V2G) being moved from down phases ($P < P_{ave}$) to up phases ($P > P_{ave}$) in order to increase power in down phases and decrease power in up phases. Based on the final stage, (24)–(27) and (33)–(36), the phase changing depends on additional powers of each phase and the number of EVs (G2V) in up phases ($P > P_{ave}$) and the number of EVs (V2G) in down phases ($P < P_{ave}$)

$$\text{Phase } z: \begin{cases} P_z - P_{\text{ave}} = P_{\text{add}-z}, N_{\text{exch}-z-\text{ini}} = \dfrac{P_{\text{add}-z}}{230 \times 10 \times 0.9}, \\ N_{\text{exch}-z-\text{lim}} = N_{\text{exch}-z-\text{ini}} \times F. \end{cases} \quad (15)$$

$$\text{Phase } x: \begin{cases} P_{\text{ave}} - P_X = P_{\text{add}-x}, N_{\text{exch}-x-\text{ini}} = \dfrac{P_{\text{add}-x}}{230 \times 10 \times 0.9}, \\ N_{\text{exch}-x-\text{lim}} = N_{\text{exch}-x-\text{ini}} \times F. \end{cases} \quad (16)$$

Phase y (first state):

$$\begin{cases} P_y - P_{\text{ave}} = P_{\text{add}-y}, N_{\text{exch}-y-\text{ini}} = \dfrac{P_{\text{add}-y}}{230 \times 10 \times 0.9}, \\ N_{\text{exch}-y-\text{lim}} = N_{\text{exch}-y-\text{ini}} \times F. \end{cases} \quad (17)$$

Phase y (second state):

$$\begin{cases} P_{\text{ave}} - P_y = P_{\text{add}-y}, N_{\text{exch}-y-\text{ini}} = \dfrac{P_{\text{add}-y}}{230 \times 10 \times 0.9}, \\ N_{\text{exch}-y-\text{lim}} = N_{\text{exch}-y-\text{ini}} \times F. \end{cases} \quad (18)$$

First state: $P_x < P_{\text{ave}}, P_y > P_{\text{ave}}, P_z > P_{\text{ave}}$

First stage:
$$\begin{cases} \text{Phase } x : P_{\text{add}-x1} = P_{\text{ave}} - P_{x1}. \\ \text{Phase } y : P_{\text{add}-y1} = P_{y1} - P_{\text{ave}}. \\ \text{Phase } z : P_{\text{add}-z1} = P_{z1} - P_{\text{ave}}. \\ P_{\text{add}-x1} = P_{\text{add}-z1} + P_{\text{add}-y1}. \end{cases} \quad (19)$$

Second stage:
$$\begin{cases} \text{Phase } x : P_{\text{add}-x2} = (P_{\text{ave}} - P_{x2}) \rightarrow P_{\text{add}-x1} > P_{\text{add}-x2}, P_{x1} < P_{x2}. \\ \text{Phase } y : P_{\text{add}-y2} = (P_{y2} - P_{\text{ave}}) \rightarrow P_{\text{add}-y1} > P_{\text{add}-y2}, P_{y1} > P_{y2}. \\ \text{Phase } z : P_{\text{add}-z2} = (P_{z2} - P_{\text{ave}}) \rightarrow P_{\text{add}-z1} > P_{\text{add}-z2}, P_{z1} > P_{z2}. \\ P_{\text{add}-x2} = P_{\text{add}-z2} + P_{\text{add}-y2}. \end{cases}$$
$$(20)$$

$$\begin{cases} \text{Phase } x : N_{\text{G2V1}} < N_{\text{G2V2}}, N_{\text{V2G1}} > N_{\text{V2G2}}. \\ \text{Phase } y : N_{\text{G2V1}} > N_{\text{G2V2}}, N_{\text{V2G1}} < N_{\text{V2G2}}. \\ \text{Phase } z : N_{\text{G2V1}} > N_{\text{G2V2}}, N_{\text{V2G1}} < N_{\text{V2G2}}. \end{cases} \quad (21)$$

$$\begin{cases} \text{Phase } x : N_{\text{exch}-\text{G2V}-x} = N_{\text{G2V2}} - N_{\text{G2V1}}, \\ N_{\text{exch}-\text{V2G}-x} = N_{\text{V2G1}} - N_{\text{V2G2}}. \\ \text{Phase } y : N_{\text{exch}-\text{G2V}-y} = N_{\text{G2V1}} - N_{\text{G2V2}}, \\ N_{\text{exch}-\text{V2G}-y} = N_{\text{V2G2}} - N_{\text{V2G1}}. \\ \text{Phase } z : N_{\text{exch}-\text{G2V}-z} = N_{\text{G2V1}} - N_{\text{G2V2}}, \\ N_{\text{exch}-\text{V2G}-z} = N_{\text{V2G2}} - N_{\text{V2G1}}. \end{cases} \quad (22)$$

$$\begin{cases} N_{\text{exch}-x} = N_{\text{exch}-\text{G2V}-x} + N_{\text{exch}-\text{V2G}-x}. \\ N_{\text{exch}-\text{G2V}-x} = N_{\text{exch}-\text{G2V}-z} + N_{\text{exch}-\text{G2V}-y}. \\ N_{\text{exch}-\text{V2G}-x} = N_{\text{exch}-\text{V2G}-z} + N_{\text{exch}-\text{V2G}-y}. \end{cases} \quad (23)$$

Ideal stage:
$$\begin{cases} \text{Phase } x \; P_{\text{add}-x-\text{fin}} = (P_{\text{ave}} - P_{x-\text{fin}}) = 0 \rightarrow P_{x-\text{fin}} = P_{\text{ave}}. \\ \text{Phase } y : P_{\text{add}-y-\text{fin}} = (P_{y-\text{fin}} - P_{\text{ave}}) = 0 \rightarrow P_{y-\text{fin}} = P_{\text{ave}}. \\ \text{Phase } z : P_{\text{add}-z-\text{fin}} = (P_{z-\text{fin}} - P_{\text{ave}}) = 0 \rightarrow P_{z-\text{fin}} = P_{\text{ave}}. \end{cases} \quad (24)$$

Subject to:
$$\begin{aligned} N_{\text{exch}-x-\text{fin}} &\le N_{\text{exch}-x-\text{lim}}, \\ N_{\text{exch}-x-\text{fin}} &\le N_{\text{G2V}(z)} + N_{\text{G2V}(y)} + N_{\text{V2G}(x)}. \end{aligned} \quad (25)$$

$$\begin{aligned} N_{\text{exch}-y-\text{fin}} &\le N_{\text{exch}-y-\text{lim}}, \\ N_{\text{exch}-y-\text{fin}} &\le N_{\text{G2V}(y)} + (\beta_1 \times N_{\text{V2G}(x)}). \end{aligned} \quad (26)$$

$$\begin{aligned} N_{\text{exch}-z-\text{fin}} &\le N_{\text{exch}-z-\text{lim}}, \\ N_{\text{exch}-z-\text{fin}} &\le N_{\text{G2V}(z)} + (\beta_2 \times N_{\text{V2G}(x)}). \end{aligned} \quad (27)$$

$$\beta_1 + \beta_2 = 1, \quad \beta_2 \ge \beta_1.$$

Second state: $P_x < P_{\text{ave}}, P_y < P_{\text{ave}}, P_z > P_{\text{ave}}$

First stage:
$$\begin{cases} \text{Phase } x : P_{\text{add}-x1} = P_{\text{ave}} - P_{x1}. \\ \text{Phase } y : P_{\text{add}-y1} = P_{\text{ave}} - P_{y1}. \\ \text{Phase } z : P_{\text{add}-z1} = P_{z1} - P_{\text{ave}}. \\ P_{\text{add}-z1} = P_{\text{add}-x1} + P_{\text{add}-y1}. \end{cases} \quad (28)$$

Second stage:
$$\begin{cases} \text{Phase } x : P_{\text{add}-x2} = (P_{\text{ave}} - P_{x2}) \rightarrow P_{\text{add}-x1} \\ \qquad > P_{\text{add}-x2}, P_{x1} < P_{x2}. \\ \text{Phase } y : P_{\text{add}-y2} = (P_{\text{ave}} - P_{y2}) \rightarrow P_{\text{add}-y1} \\ \qquad > P_{\text{add}-y2}, P_{y1} < P_{y2}. \\ \text{Phase } z : P_{\text{add}-z2} = (P_{z2} - P_{\text{ave}}) \rightarrow P_{\text{add}-z1} \\ \qquad > P_{\text{add}-z2}, P_{z1} < P_{z2}. \\ P_{\text{add}-z2} = P_{\text{add}-x2} + P_{\text{add}-y2}. \end{cases} \quad (29)$$

$$\begin{cases} \text{Phase } x : N_{\text{G2V1}} < N_{\text{G2V2}}, N_{\text{V2G1}} > N_{\text{V2G2}}. \\ \text{Phase } y : N_{\text{G2V1}} < N_{\text{G2V2}}, N_{\text{V2G1}} > N_{\text{V2G2}}. \\ \text{Phase } z : N_{\text{G2V1}} < N_{\text{G2V2}}, N_{\text{V2G1}} > N_{\text{V2G2}}. \end{cases} \quad (30)$$

$$\begin{cases} \text{Phase } x : N_{\text{exch}-\text{G2V}-x} = N_{\text{G2V2}} - N_{\text{G2V1}}, \\ N_{\text{exch}-\text{V2G}-x} = N_{\text{V2G1}} - N_{\text{V2G2}}. \\ \text{Phase } y : N_{\text{exch}-\text{G2V}-y} = N_{\text{G2V2}} - N_{\text{G2V1}}, \\ N_{\text{exch}-\text{V2G}-y} = N_{\text{V2G1}} - N_{\text{V2G2}}. \\ \text{Phase } z : N_{\text{exch}-\text{G2V}-z} = N_{\text{G2V1}} - N_{\text{G2V2}}, \\ N_{\text{exch}-\text{V2G}-z} = N_{\text{V2G2}} - N_{\text{V2G1}}. \end{cases} \quad (31)$$

$$\begin{cases} N_{\text{exch}-z} = N_{\text{exch}-\text{G2V}-z} + N_{\text{exch}-\text{V2G}-z}. \\ N_{\text{exch}-\text{G2V}-z} = N_{\text{exch}-\text{G2V}-x} + N_{\text{exch}-\text{G2V}-y}. \\ N_{\text{exch}-\text{V2G}-z} = N_{\text{exch}-\text{V2G}-x} + N_{\text{exch}-\text{V2G}-y}. \end{cases} \quad (32)$$

Ideal stage
$$\begin{cases} \text{Phase } x : P_{\text{add}-x-\text{fin}} = (P_{\text{ave}} - P_{x-\text{fin}}) = 0 \rightarrow P_{x-\text{fin}} = P_{\text{ave}}. \\ \text{Phase } y : P_{\text{add}-y-\text{fin}} = (P_{\text{ave}} - P_{y-\text{fin}}) = 0 \rightarrow P_{y-\text{fin}} = P_{\text{ave}}. \\ \text{Phase } z : P_{\text{add}-z-\text{fin}} = (P_{z-\text{fin}} - P_{\text{ave}}) = 0 \rightarrow P_{z-\text{fin}} = P_{\text{ave}}. \end{cases} \quad (33)$$

Subject to
$$\begin{aligned} N_{\text{exch}-z-\text{fin}} &\le N_{\text{exch}-z-\text{lim}}, \\ N_{\text{exch}-z-\text{fin}} &\le N_{\text{V2G}(x)} + N_{\text{V2G}(y)} + N_{\text{G2V}(z)}. \end{aligned} \quad (34)$$

$$\begin{aligned} N_{\text{exch}-y-\text{fin}} &\le N_{\text{exch}-y-\text{lim}}, \\ N_{\text{exch}-y-\text{fin}} &\le N_{\text{V2G}(y)} + (\beta_1 \times N_{\text{G2V}(z)}). \end{aligned} \quad (35)$$

$$\begin{aligned} N_{\text{exch}-x-\text{fin}} &\le N_{\text{exch}-x-\text{lim}}, \\ N_{\text{exch}-x-\text{fin}} &\le N_{\text{V2G}(x)} + (\beta_2 \times N_{\text{G2V}(z)}). \end{aligned} \quad (36)$$

$$\beta_1 + \beta_2 = 1, \quad \beta_2 \ge \beta_1.$$

Again, in the second stage, factors β_1 and β_2 are weight factors that are used for phase changing of EVs between different phases. In fact, these factors determine portions of EVs (G2V) of phase (z) in balancing of phases (x), (y) and their amount depends on the PC of phases.

2.5 Charging scenarios for EVs (G2V–V2G)

For investigating the effect of EVs presence on different priorities, the scenarios have been defined as various presence per cent on network parameters such as power consumption, power losses, and voltage profile. The on-peak and off-peak times of network loads play a critical role in determining time priorities. Based on human patterns, the home-like customers go to their home at 17:00 h and they leave for work the next day at 7:00 h [29, 30]. The time of EVs arrival is at 17:00 h and the time of EVs departure is at 7:00 h. First-time priority is synchronous with the peak time of network (17:00–24:00 h) and it has the highest fee for getting power (G2V) and injecting power (V2G) to the network due to SLMC servicing EVs in the peak period of the network. The second time priority is synchronous with the peak time of network (17:00–24:00 h) and, it

Table 1 EVs charging scenarios

Scenarios		Charging time (scheme) (15 min)
first	(A)	uncoordinated random (G2V) charging over (17:00–24:00 h)
	(B)	coordinated random (G2V) charging over (17:00–24:00 h)
	(C)	coordinated random (G2V) and(V2G) charging over (17:00–24:00 h)
second	(A)	uncoordinated random (G2V) charging over (17:00–7:00 h)
	(B)	coordinated random (G2V) charging over (17:00–7:00 h)
	(C)	coordinated random (G2V) and(V2G) charging over (17:00–7:00 h)
third	(A)	uncoordinated random (G2V) charging over (24:00–7:00 h)
	(B)	coordinated random (G2V) charging over (24:00–7:00 h)
	(C)	coordinated random (G2V) and(V2G) charging over (24:00–7:00 h)
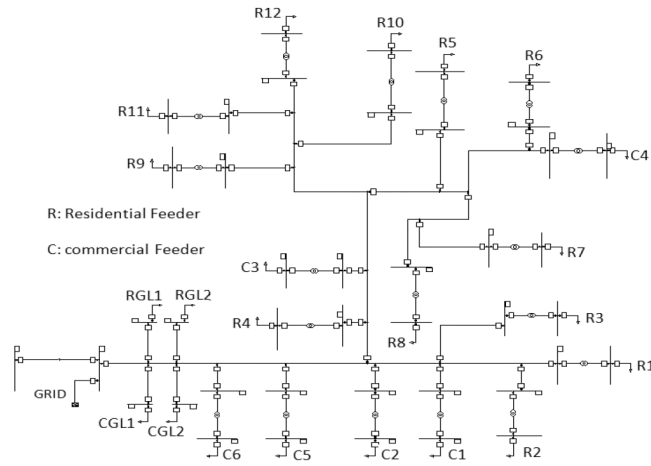
Fig. 5 *Smart unbalanced distribution system includes 20 kV and 400 V networks and unbalanced residential and commercial loads and distribution transformers [28]*

has the lowest fee getting power (G2V) and injection power (V2G) to network due to SLMC servicing EVs in an off-peak period of network and perhaps these services are not needed in time intervals.

In Table 1, the charging scenarios are presented.

Time priorities play a critical role in determining three scenarios of EVs charging (G2V, V2G). According to the first scenario, EVs connect to the network in the first-time priority (between 17:00 and 24:00 h) and that is synchronous with the peak period of loads.

In the second scenario, EVs are connected to the network (plug-in) during first- and second-time priorities between 17:00 and 7:00 h. This scenario is the closest to illustrating an actual state of the network. In the third scenario, EVs are joined to the network during the second time priority between 24:00 and 7:00 h and this scenario corresponds to the off-peak period of loads.

Implementation of the suggested algorithm has been performed in the Ilam distribution system (20 kV–400 V) [27, 28]. The grid includes unbalanced loads of residential and commercial applications, containing 12 residential feeders (20 kV–400 V) and six commercial feeders, which have been illustrated in Fig. 5 [28].

The algorithm has been programmed and simulated with DPL in Digsilent software [31]. For the simulation of EVs, the Mitsubishi EVs (i-MiEV) have been selected with 16 kWh battery capacity [32]. The final state of charge (SOC) of EV (G2V) is about 90% during 7 h and primary SOC of EV is about 5% and this level of charging (90%) is enough (gets 85% energy from grid) and

the primary SOC of EV (V2G) is about 90% and the final SOC of EV is about 5% (injects 85% energy to grid). The charging rate of the charger is always the same. Masoum *et al.* [29] offered that the network maximum demand ($D_{\Delta t,\max}$) is 5% or 10% greater than the maximum power consumption of the network without EVs (due to transformer capacity: 63–20 kV).

3 Simulation results

In this part, the results of network analysis are shown as follows. In the first section, PEVs (G2V) connect to a network as random according to three scenarios. After that, the proposed algorithm coordinates the scheme of PEVs charging. Finally, PEVs (G2V, V2G) connect to a network and a charging scheme is managed by the proposed algorithm in the second section.

3.1 Presence of EVs (G2V) in three different scenarios

Fig. 6 shows TPPC in the first scenario (with 100% EV penetration) considering two states. The blue, green and red lines are power consumptions of the phases *R*, *S*, and *T*, respectively, before the implementation of the suggested algorithm. For 24 h, there is a considerable unbalanced condition, especially between 17:00 and 23:00 when the EVs are integrated and the PCs are at the highest level, as shown in Fig. 6. The mentioned differences in TPPC are due to the reduction of the EVs presence and decreasing on the PC between 01:00 and 05:00. From 05:00, unbalanced distance of three-phase power consumption (UDTTPC) has risen.
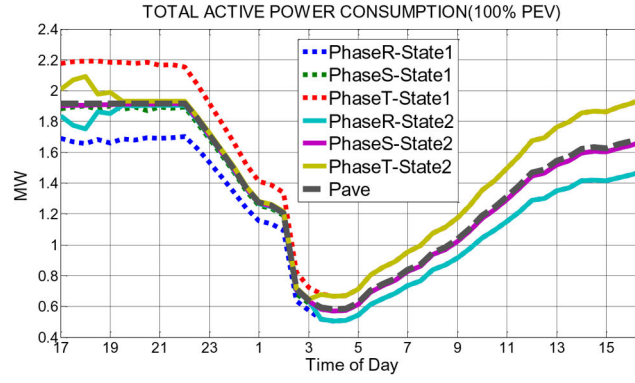
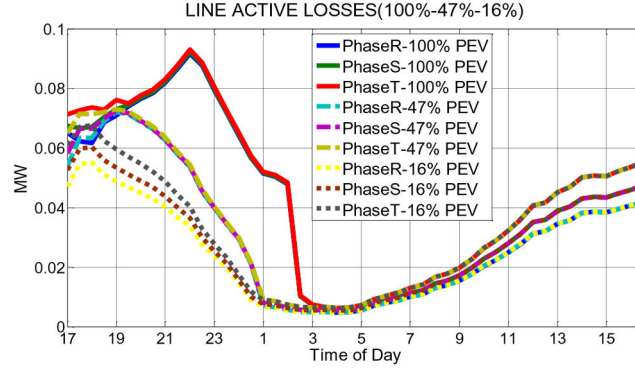**Fig. 6** *State B of the first scenario-TPPC in 100% penetration before and after utilisation of the algorithm*

Fig. 7 *State B of the first scenario-active line losses in different penetrations*
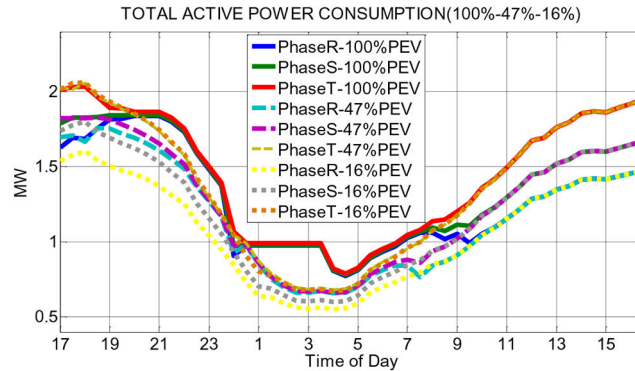

Fig. 8 *State B of the second scenario-TPPC in different penetrations*

In the second state, the dotted line represents the average power of three phases (APTP) throughout 24 h, i.e. the real amount for all phases. By using the new algorithm, where dark blue, pink, and yellow lines, which are PCs of phases *R*, *S*, and *T*, TPPC is seriously close to APTP and unbalanced distances in powers are removed in these times. In spite of this, there are some fluctuations at initial times because of EVs presence and TPC limitations between 17:00 and 03:00. Since the EVs integration is at the highest level after 22:00, by plugging out EVs and growth of base PC after 03:30, UDTTPC has collapsed and trends of the second state are on their first state. Generally, the green line of the first state and pink line of the second state (which represents the phase S of the grid), are close to APTP due to the basic PC. The successful performance of the new algorithm is shown in the initial times of the first scenario as the UDTTPC has declined with the increasing number of EVs. Fig. 7 reveals active power line losses in the first situation after the utilisation of the new algorithm (EVs penetration level are: 16, 47, and 100%). As shown, from 17:00 to 3:00 am, the unbalanced distances of three-phase losses (such as TPPC) decreased. The power losses in three phases have been lifted, because of the increasing base power consumption and the number of EVs. However, in 16% of penetration level, the unbalanced condition is clear, as a result of a smaller number of EVs. Fig. 8 shows TPPC in the second scenario. While an

unbalanced load has been removed at 01:00, the active power losses decrease by plugging out EVs at 03:00. In this scenario, UDTTPC is apparent (especially 16% of the penetration level) due to several EVs (G2V) after 12:00. With the integration of many EVs at 22:00, UDTTPC has been drastically reduced with the high level of EVs penetration.

From 24:00, UDTTPC has been removed in 100% penetration level of EVs and it has decreased to 47% penetration level of EVs, only in 16% it is clear. It is obvious that during the periods of 17:00–21:00 and 24:00–4:00 am, TPPC is constant in 100% penetration level due to performing TPC limitations [28] by the algorithm in these times. TPPC is presented in Fig. 9 in the third scenario, which EVs are connected to the grid from 24:00. In this case, there is a considerable unbalanced distance. Owing to the high level of EVs and low level of basic PC, UDTTPC has been approximately removed in all EVs with a 100% penetration level between 24:00 and 06:00 because of the high level of EVs compared to other penetrations. In addition, UDTTPC will drastically increase by plugging out EVs and increasing of PC. Between 24:00 and 06:00, TPPC is constant due to TPC limitations. However, TPPC has a considerable jump from 6:00 am. Table 2 shows unbalanced percentages of three phases in three scenarios before and after usage of the new algorithm.
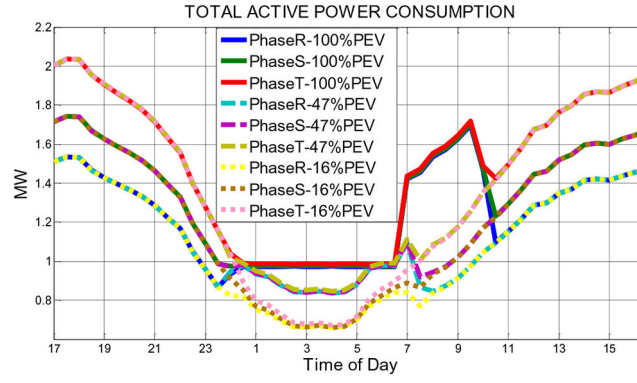
Fig. 9 *State B of the third scenario-TPPC in different penetrations*

Table 2 Unbalanced percentages of network phases before (state 1) and after (state 2) utilisation of algorithm in EVs (G2V)

Scenario	G2V, %		State 1	
		$\text{Unb}_R\%$	$\text{Unb}_S\%$	$\text{Unb}_T\%$
first	100	11.2863	1.5629	12.8492
	47	12.3067	1.1727	13.4795
	16	13.2896	1.08730	14.3769
second	100	11.7011	1.58503	13.2862
	47	12.7734	0.87088	13.6315
	16	13.2728	1.48574	14.7585
third	100	10.3515	1.51695	11.8587
	47	10.8102	1.05571	11.8659
	16	13.0204	1.65096	14.6714

Scenario	G2V, %		State 2	
		$\text{Unb}_R\%$	$\text{Unb}_S\%$	$\text{Unb}_T\%$
first	100	1.66807	0.28807	1.9488
	47	4.31960	0.56901	4.88861
	16	10.1799	0.97494	11.1548
second	100	2.16402	0.39963	2.56366
	47	5.31583	0.61897	5.92204
	16	10.7267	1.28824	12.0150
third	100	1.51541	0.26950	1.77520
	47	4.05356	0.61659	4.67015
	16	7.33955	1.06053	8.40008

Generally, the unbalanced per cent of phase T is more than the two other phases and unbalanced percentage of phase S is less than the other phases. Of course, unbalanced percentages of the first and second scenarios are more than the third one. In the same way, unbalanced percentage of the third scenario has decreased more than other scenarios. By increasing EVs levels, unbalanced percentages of this scenario have noticeably declined compared to the last case. The most reduction of unbalanced percentage is related to 100% EVs in the third scenario: unbalanced present fell from 10.53 to 1.51% in phase R and 1.516 to 0.256% in phase S and in phase T, from 11.85 to 1.775%, respectively. In general, the results indicated that the performance of the new algorithm is acceptable and great in different scenarios

$$P_{\text{ave}} = \frac{P_R + P_S + P_T}{3}, \quad \text{Unb}_R\% = \frac{P_R - P_{\text{ave}}}{P_{\text{ave}}}, \quad (37)$$

$$\text{Unb}_S\% = \frac{P_S - P_{\text{ave}}}{P_{\text{ave}}}, \quad \text{Unb}_T\% = \frac{P_T - P_{\text{ave}}}{P_{\text{ave}}}, \quad (38)$$

3.2 Presence of PEV (G2V–V2G) in three scenarios

Fig. 10 illustrates TPPC in the first scenario by the presence of G2V–V2G at the same time. UDTTPC has been removed from

17:00 to 24:00 by plugging in (G2V–V2G). Also, by increasing the presence of V2G and decreasing the presence of G2V, TPPC has reduced as the TPPC of (47% G2V–16% V2G) EVs is more than TPPC of (32% G2V–32% V2G). With a 16% decrease in G2V and a 16% increase in V2G, TPPC will reduce in the same way. According to trends, UDTTPC reduced equally in all three scenarios because the number of EVs is the same (64% EVs) in all scenarios. Of course, there are some power fluctuations in three phases from 17:00 to 18:00 because of EVs random plugins and the PC of some phases is constant (TPC limitations). By plugging out EVs (G2V–V2G) from hour 24, UDTTPC will appear and trends of all penetrations are about the same. In Fig. 11, according to the second scenario, the plugging in of EVs is from 17:00 to 07:00 and UDTTPC are removed. TPPC has fluctuated because of the random presence of EVs (G2V) in (47% G2V–16% V2G) and TPC limitations [28]. From 7 am (such as previous cases) by plugging out EVs, UDTTPC will appear. Finally, there will be unbalanced conditions in different parameters beginning at 07:00 once EVs are disconnected. The unbalanced percentages of three phases in three scenarios can be seen in Table 3. Generally, the decreased percentages of unbalancing in three phases (R, S, and T) are approximately the same in three presence percentages, especially in the third scenario. Of course, unbalancing in (32% G2V–32% V2G) decreased more than other penetrations in all scenarios. Based on the last case, phase S has minimum unbalancing and
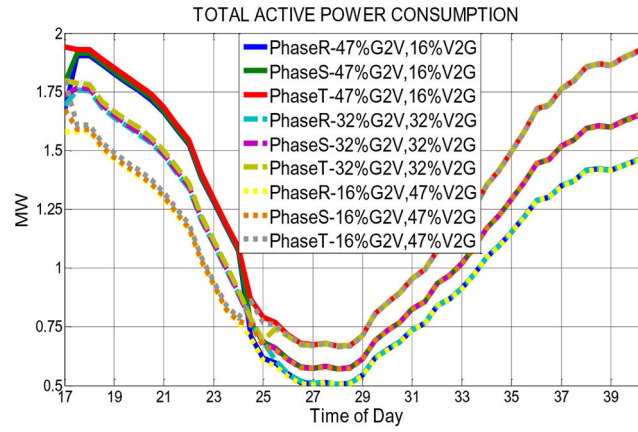
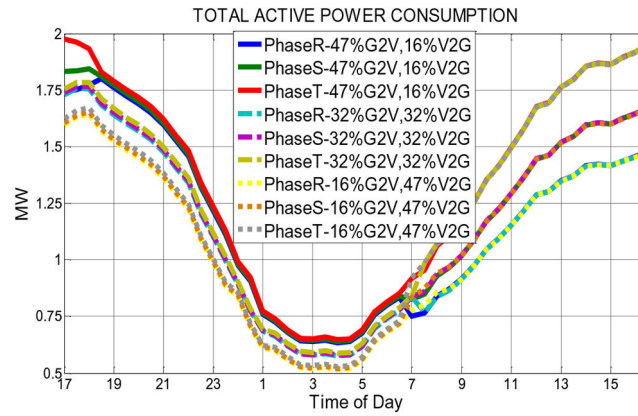**Fig. 10** *State C of first scenario-TPPC in different penetrations*

Fig. 11 *State C of second scenario-TPPC in different penetrations*

Table 3 Unbalanced percentages of network phases before (state 1) and after (state 2) utilisation of algorithm in EVs (G2V–V2G)

Scenario	G2V, %	G2V, %	State1		
			$Unb_R\%$	$Unb_S\%$	$Unb_T\%$
first	100	16	11.4024	1.71772	13.1201
	47	32	13.0724	1.63715	14.7096
	16	47	14.3967	2.9271	17.3238
second	100	16	13.1645	1.43622	14.6007
	47	32	12.7806	1.81288	14.5935
	16	47	14.1627	2.22165	16.3844
third	100	16	12.3622	0.5099	12.7374
	47	32	13.9063	0.83562	14.7392
	16	47	15.5191	2.59261	18.1117

Scenario	G2V, %	V2G, %	State2		
			$Unb_R\%$	$Unb_S\%$	$Unb_T\%$
first	100	16	3.69715	0.62849	4.32564
	47	32	2.86737	0.52446	3.39183
	16	47	3.83694	0.68451	4.52145
second	100	16	2.72927	0.37254	3.10181
	47	32	1.12578	0.2282	1.35405
	16	47	2.3103	0.43254	2.7429
third	100	16	3.14300	0.41208	3.42033
	47	32	2.75216	0.44879	3.19828
	16	47	3.12138	0.62972	3.75110

phase T has a maximum unbalancing. Finally, the mentioned algorithm has taken advantage from the opportunity of EVs presence in order to balance loads of network and perform limitations of the network (TPC, voltage profile) only by considering the total number of EVs (G2V–V2G) together and without attention to presence percentages of G2V and V2G separately.

4 Conclusion

This study suggests a new procedure to balance loads of distribution systems in order to prevent generalisation of destructive effects on the primary distribution system (external grid) and their instruments (lines, transformers, etc.) by maintaining previous abilities (TPC constraints, voltage deviations). At SLMC's first view, the presence of EVs (G2V, V2G) is a serious threat to the security and instruments of the network. However, the proposed algorithm has converted the improper condition to an opportunity advantage (optimal method because of MSS, high speed of processing). Moreover, new benefits have been obtained on account of LB by considering the number of EVs (G2V, V2G) without attention to the type of EV. The results confirmed the appropriate and effective performance of the algorithm in the real-time domain during implementation in different scenarios. It is clear by growing the penetrations of EVs, proficiency, and abilities of the procedure are more significant and more obvious. With the presence of EVs (G2V) in three scenarios, UDTTPC diminished more in the third scenario compared with the first and second scenarios because of the conditions of networks and EVs in this scenario. In a 100% penetration level, the best results have been obtained in all scenarios. Also, in the presence of EVs (G2V, V2G), UDTTPC is the least amount in the second scenario, although the amount of reduction of UDTTPC in different scenarios is approximately equal to all scenarios' quantity despite some fluctuations.

5 References

[1] Mukherjee, J.C., Gupta, A.: 'Distributed charge scheduling of plug-in electric vehicles using inter-aggregator collaboration', *IEEE Trans. Smart Grid*, 2017, **8**, (1), pp. 331–341

[2] Ismail, M., Bayram, I.S., Abdallah, M.*, et al.*: 'Optimal planning of fast PEV charging facilities'. IEEE Smart Grid and Renewable Energy, Doha, Qatar, March 2015, pp. 1–6

[3] Wang, X., Yuen, C., Hassan, N.U.*, et al.*: 'Electric vehicle charging station placement for urban public bus systems', *IEEE Trans. Intell. Transp. Syst.*, 2017, **18**, (1), pp. 128–139

[4] Xu, H., Miao, S., Zhang, C.*, et al.*: 'Optimal placement of charging infrastructures for large-scale integration of pure electric vehicles into grid', *Int. J. Electr. Power Energy Syst.*, 2013, **53**, (1), pp. 159–165

[5] Pazouki, S., Mohsenzadeh, A., Ardalan, S.*, et al.*: 'Simultaneous planning of PEV charging stations and DGs considering financial, technical, and environmental effects', *Can. J. Electr. Comput. Eng.*, 2015, **38**, (3), pp. 238–245

[6] Mohsenzadeh, A., Pang, C., Pazouki, S.*, et al.*: 'Optimal siting and sizing of electric vehicle public charging stations considering smart distribution network reliability'. North American Power Symp., Charlotte, USA, October 2015, pp. 1–6

[7] Zhang, H., Hu, Z., Xu, Z.*, et al.*: 'Optimal planning of PEV charging station with single output multiple cables charging spots', *IEEE Trans. Smart Grid*, 2017, **PP**, (99), pp. 1–10

[8] Luo, C., Huang, Y., Gupta, V.: 'Stochastic dynamic pricing for EV charging stations with renewable integration and energy storage', *IEEE Trans. Smart Grid*, 2018, **9**, (2), pp. 1494–1505

[9] Karfopoulos, L., Hatziargyriou, N.: 'Distributed coordination of electric vehicles providing V2G services', *IEEE Trans. Power Syst.*, 2016, **31**, (1), pp. 329–338

[10] Masoum, S., Deilami, S., Moses, P.S.*, et al.*: 'Smart load management of plug-in electric vehicles in distribution and residential networks with charging stations for peak shaving and loss minimisation considering voltage regulation', *IET Gener. Transm. Distrib.*, 2010, **5**, (8), pp. 877–888

[11] Sortomme, E., Hindi, M.M., MacPherson, S.D.J.*, et al.*: 'Coordinated charging of plug-in hybrid electric vehicles to minimize distribution system losses', *IEEE Trans. Smart Grid*, 2011, **2**, (1), pp. 198–205

[12] Tal, G., Nicholas, M., Davies, J.*, et al.*: 'Charging behavior impacts on electric vehicle miles traveled: who is not plugging in?', *Transp. Res. Rec. J. Transp. Res. Board*, 2014, **2454**, (2454), pp. 53–60

[13] Clement-Nyns, K., Haesen, E., Driesen, J.: 'The impact of charging plug-in hybrid electric vehicles on a residential distribution grid', *IEEE Trans. Power Syst.*, 2010, **25**, (1), pp. 371–380

[14] Kejun, Q., Chengke, Z., Allan, M.*, et al.*: 'Modeling of load demand due to EV battery charging in distribution systems', *IEEE Trans. Power Syst.*, 2011, **26**, (2), pp. 802–810

[15] Gan, L., Topcu, U., Low, S.: 'Optimal decentralized protocol for electric vehicle charging', *IEEE Trans. Power Syst.*, 2013, **28**, (2), pp. 940–951

[16] Juanuwattanakul, P., Masoum, M.A.S.: 'Increasing distributed generation penetration in multiphase distribution networks considering grid losses, maximum loading factor and bus voltage limits', *IET Gener. Transm. Distrib.*, 2012, **6**, (12), pp. 1262–1271

[17] Tan, K.M., Ramachandaramurthy, V.K., Yong, J.Y.: 'Integration of electric vehicles in smart grid: a review on vehicle to grid technologies and optimization techniques', *Renew. Sustain. Energy Rev.*, 2016, **53**, pp. 720–732

[18] El-Zonkoly, A.: 'Intelligent energy management of optimally located renewable energy systems incorporating PHEV', *Energy Convers. Manage.*, 2014, **84**, pp. 427–435

[19] Al-Awami, A.T., Sortomme, E.: 'Coordinating vehicle-to-grid services with energy trading', *IEEE Trans. Smart Grid*, 2012, **3**, (1), pp. 453–462

[20] Sexauer, J.M., McBee, K.D., Bloch, K.A.: 'Applications of probability model to analyze the effects of electric vehicle chargers on distribution transformers', *IEEE Trans. Power Syst.*, 2013, **28**, (2), pp. 847–854

[21] Yan, Q., Kezunovic, M.: 'Impact analysis of electric vehicle charging on distribution system'. 2012 North American Power Symp. (NAPS), Champaign, Illinois (IL), USA, September 2012, pp. 1–6

[22] Wei, W., Wu, L., Wang, J.*, et al.*: 'Expansion planning of urban electrified transportation networks: a mixed-integer convex programming approach', *IEEE Trans. Transp. Electrif.*, 2017, **3**, (1), pp. 210–224

[23] Luo, C., Huang, Y.-F., Gupta, V.: 'A consumer behavior based approach to multistage EV charging station placement'. 81st IEEE Vehicular Technology Conf. (VTC Spring), Glasgow, UK, 2015, pp. 1–6

[24] Geng, B., Mills, J.K., Sun, D.: 'Two-stage charging strategy for plug-in electric vehicles at the residential transformer level', *IEEE Trans. Smart Grid*, 2013, **4**, (3), pp. 1442–1452

[25] Chenrui, J., Jian, T., Ghosh, P.: 'Optimizing electric vehicle charging with energy storage in the electricity market', *IEEE Trans. Smart Grid*, 2013, **4**, (1), pp. 311–320

[26] Rotering, N., Ilic, M.: 'Optimal charge control of plug-in hybrid electric vehicles in deregulated electricity markets', *IEEE Trans. Power Syst.*, 2011, **26**, (3), pp. 1021–1029

[27] The information and data of electricity distribution company of Ilam, Ilam-Iran, April 2013

[28] Hajizadeh, A., Kikhavandi, M.: 'Coordination of bidirectional charging for plug-in electric vehicles in smart distribution systems', *Electr. Eng.*, 2018, **100**, (2), pp. 1085–1096

[29] Deilami, S., Masoum, A.S., Moses, P.S.: 'Real-time coordination of plug-in electric vehicle charging in smart grids to minimize power losses and improve voltage profile', *IEEE Trans. Smart Grid*, 2011, **2**, (3), pp. 456–467

[30] Li, G., Zhang, X.-.P.: 'Modeling of plug-in hybrid electric vehicle charging demand in probabilistic power flow calculations', *IEEE Trans. Smart Grid*, 2012, **3**, (1), pp. 492–499

[31] Digsilent software (2013) Demo version 13.1. Available at http://www.digsilent.com/

[32] Mitsubishi (2013) Electric car (i-MiEV). Available at http://www.mitsubishimotors.com.au/vehicles/i-miev